

# Colorimetric Sensor Array for Determination and Identification of Toxic Industrial Chemicals

Liang Feng,<sup>†</sup> Christopher J. Musto,<sup>†</sup> Jonathan W. Kemling,<sup>†</sup> Sung H. Lim,<sup>§</sup> Wenxuan Zhong,<sup>‡</sup> and Kenneth S. Suslick<sup>\*,†</sup>

Department of Chemistry, University of Illinois at Urbana–Champaign, 600 S. Mathews Avenue, Urbana, Illinois 61801, United States, Department of Statistics, University of Illinois at Urbana–Champaign, 725 S. Wright Street, Champaign, Illinois 61820, United States, and iSense, LLC, 470 Ramona Street, Palo Alto, California 94301, United States

A low-cost yet highly sensitive colorimetric sensor array for the detection and identification of toxic industrial chemicals (TICs) has been developed. The sensor consists of a disposable array of cross-responsive nanoporous pigments whose colors are changed by diverse chemical interactions with analytes. Clear differentiation among 20 different TICs has been easily achieved at both their IDLH (immediately dangerous to life or health) concentration within 2 min of exposure and PEL (permissible exposure limit) concentration within 5 min of exposure with no errors or misclassifications. Detection limits are generally well below the PEL (in most cases below 5% of PEL) and are typically in the low ppb range. The colorimetric sensor array is not responsive to changes in humidity or temperature over a substantial range. The printed arrays show excellent batch to batch reproducibility and long shelf life (greater than 3 months).

Toxic industrial chemicals, by their very nature, are chemically reactive. The toxicities inherent in toxic industrial chemicals derive from a very wide range of specific chemical reactivities that affect multiple systems within living organisms. Some acute toxins target specific, critical metabolic enzymes (e.g., HCN inhibits cytochrome c oxidase while phosgene inhibits pulmonary function); some cause cell lysis in the lungs creating pulmonary edema (e.g., HCl, HF), and others are potent oxidants or reductants that can target various biosystems.

Current electronic nose technology<sup>1</sup> generally relies on sensors whose responses originate from weak and highly nonspecific chemical interactions that either induce changes in physical properties (e.g., mass, volume, conductivity) or follow after physisorption on surfaces (e.g., analyte oxidation on heated metal oxides). Specific examples of such sensors include conductive polymers and polymer composites, multiple polymers doped with fluorescent dyes, polymer coated surface acoustic wave (SAW) devices, and metal oxide sensors. On the basis of these types of sensors, array-based sensing technology has proven to be a potentially powerful approach toward the detection of chemically diverse analytes.

Despite their successes, current technologies have a limited ability to detect compounds at low concentrations relative to analyte saturation vapor pressure and are often unable to discriminate among similar compounds within a chemical class. In addition, interference from large environmental changes in humidity or temperature remains highly problematic. Most of these technologies rely on weak and nonspecific chemical interactions, primarily van der Waals and physical adsorption interactions, which prohibit the development of chemical sensors with both high sensitivity and high selectivity. Furthermore, it is exceptionally difficult to increase the sensitivity of sensors while keeping them environmentally robust because an increase in sensitivity inherently leads to an increased probability of sensor poisoning during use.<sup>2</sup>

Detection of and discrimination among a wide range of high priority toxic industrial chemicals remains a particularly important but difficult challenge.<sup>3</sup> Electronic nose technology has, of course, been applied to this task. For example, Hammond et al.<sup>4</sup> recently reported on toxic industrial chemical (TIC) identification using an array of ceramic metallic films able to differentiate ten TICs with an error rate of ~10% using linear discriminant analysis. Using metal-oxide detectors combined with temperature programming, Meier et al.<sup>5</sup> examined five TICs and were able to reduce their error rate (both false negatives and positives) to 3%. Given the range of TICs with which one must be concerned and the

- (1) (a) Gardner, J. W.; Bartlett, P. N. *Electronic Noses: Principles and Applications*; Oxford University Press: New York, 1999. (b) Janata, J.; Josowicz, M. *Nat. Mater.* **2003**, *2*, 19–24. (c) Lewis, N. S. *Acc. Chem. Res.* **2004**, *37*, 663–672. (d) Hsieh, M.-D.; Zellers, E. T. *Anal. Chem.* **2004**, *76*, 1885–1895. (e) Walt, D. R. *Anal. Chem.* **2005**, *77*, 45 A. (f) Anslyn, E. V. *J. Org. Chem.* **2007**, *72*, 687–699. (g) Falconi, C.; Martinelli, E.; Di Natale, C.; D'Amico, A.; Maloberti, F.; Malcovati, P.; Baschiroto, A.; Stornelli, V.; Ferri, G. *Sens. Actuators, B: Chem.* **2007**, *121*, 295–329. (h) Borisov, S. M.; Wolfbeis, O. S. *Chem. Rev.* **2008**, *108*, 423–461. (i) Röck, F.; Barsan, N.; Weimar, U. *Chem. Rev.* **2008**, *108*, 705–725. (j) Hierlemann, A.; Gutierrez-Osuna, R. *Chem. Rev.* **2008**, *108*, 563–613. (k) Walt, D. R.; Aernicke, M. J.; Guo, J.; Sonkusale, S. *Anal. Chem.* **2009**, *81*, 5281–5290. (l) Wilson, A. D.; Baietto, M. *Sensors* **2009**, *9*, 5099–5148. (m) Meier, D. C.; Raman, B.; Semancik, S. *Annu. Rev. Anal. Chem.* **2009**, *2*, 463–484. (n) Berna, A. *Sensors* **2010**, *10*, 3882–3910. (o) Stich, M. I. J.; Fischer, L. H.; Wolfbeis, O. S. *Chem. Soc. Rev.* **2010**, *39*, 3102–3114.
- (2) (a) Suslick, K. S.; Bailey, D. P.; Ingison, C. K.; Janzen, M.; Kosal, M. A.; McNamara, W. B., II; Rakow, N. A.; Sen, A.; Weaver, J. J.; Wilson, J. B.; Zhang, C.; Nakagaki, S. *Quim. Nova* **2007**, *30*, 677–681. (b) Suslick, K. S. *MRS Bull.* **2004**, *29*, 720–725.
- (3) Hill, H. H.; Martin, S. J. *Pure Appl. Chem.* **2002**, *74*, 2281–2291.
- (4) Hammond, M. H.; Johnson, K. J.; Rose-Pehrsson, S. L.; Ziegler, J.; Walker, H.; Caudy, K.; Gary, D.; Tillett, D. *Sens. Actuators, B* **2006**, *116*, 135–144.

\* Corresponding author. Tel: 1-217-333-2794. E-mail: ksuslick@illinois.edu.

<sup>†</sup> Department of Chemistry, University of Illinois at Urbana–Champaign.

<sup>‡</sup> Department of Statistics, University of Illinois at Urbana–Champaign.

<sup>§</sup> iSense, LLC.

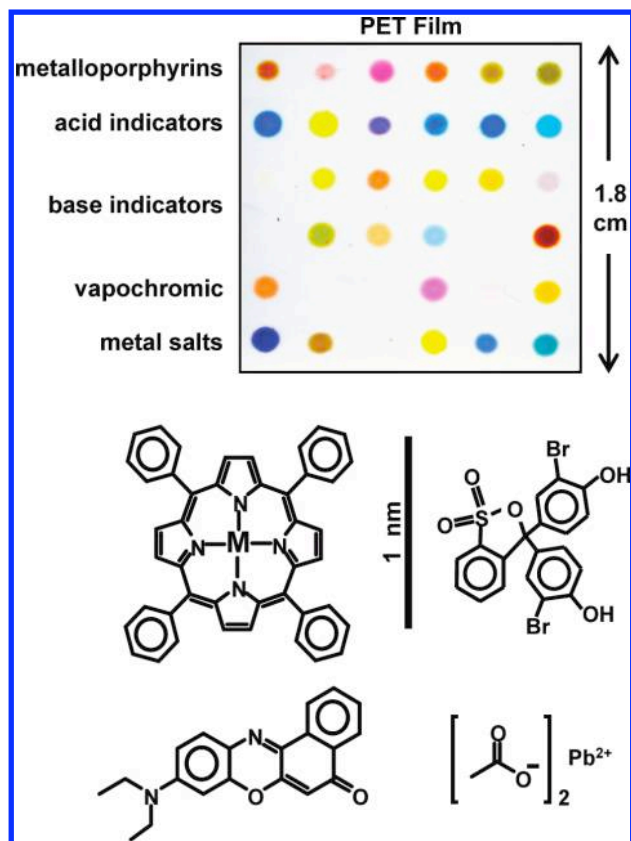


**Figure 1.** Colorimetric sensor array consisting of 36 different chemically responsive pigments which have been printed on a nonporous, polyethylene terephthalate (PET) film. Examples of each dye class are shown. The 36 dyes (some of which appear colorless before exposure) were selected empirically based on the quality of their color response to a representative selection of different analytes.

importance of very low error rates, it is clear that the inexpensive, reliable, and portable detection of toxic vapors remains an unsolved problem.

We have previously reported a general approach to an “opto-electronic nose” based on colorimetric array detection using a diverse range of chemically responsive dyes.<sup>2,6</sup> The design of our disposable colorimetric sensor array is based on dye–analyte interactions that are stronger than those that cause simple physical adsorption. The selected chemically responsive dyes fall into four classes (Figure 1): (1) dyes containing metal ions (e.g., metalloporphyrins) that respond to Lewis basicity (that is, electron-pair donation, metal-ion ligation), (2) pH indicators that respond to Brønsted acidity/basicity (that is, proton acidity and hydrogen bonding), (3) dyes with large permanent dipoles (e.g., vapochemical or solvatochromic dyes) that respond to local polarity, and

(4) metal salts that participate in redox reactions. This colorimetric sensor array, therefore, is responsive to the chemical reactivity of analytes, rather than to their effects on secondary physical properties (e.g., mass, conductivity, adsorption, etc.).

We have very recently improved our array methodology by the use of chemically responsive nanoporous pigments created from the immobilization of dyes in organically modified siloxanes (ormosils).<sup>7–9</sup> Nanoporous ormosils were chosen as the host materials for the colorants due to their high surface area, relative inertness in both gases and liquids, good stability over a wide range of pH, and optical transparency. In addition, the physical and chemical properties of the matrix (e.g., hydrophobicity, porosity) can be easily modified by changing the sol–gel formulations. The use of nanoporous pigments significantly improves the stability and shelf life of the colorimetric sensor arrays and permits direct printing onto nonpermeable polymer surfaces,<sup>7</sup> which substantially improves the ease of manufacturing the arrays. Finally, we observe that the porous matrix serves as a preconcentrator, thereby improving the overall sensitivity.<sup>8</sup>

We have recently reported the use of nanoporous pigments for the identification of many toxic gases.<sup>8</sup> Here, we report an extension of that work for colorimetric identification and semi-quantitative analysis of 20 different toxic industrial chemicals (TICs) even at very low concentrations, typically below 5% of permissible exposure limits. The TICs selected for these studies were classified as “High Hazard TICs” according to the NATO International Task Force 25 and 40,<sup>11</sup> as given in Table 1. The limits of detection and response times to the most important TICs have been tested as well as the potential effects of various interfering agents.

## EXPERIMENTAL SECTION

All reagents were of analytical-reagent grade, obtained from Sigma-Aldrich, and used as received without further purification unless otherwise specified. Certified, premixed gas tanks, including ammonia, methylamine, dimethylamine, trimethylamine, HCl, SO<sub>2</sub>, fluorine, chlorine, phosphine, arsine, phosgene, hydrogen sulfide, hydrogen cyanide, and diborane were obtained from Matheson Tri-Gas Corp. through S. J. Smith, Co. (Urbana, IL). The colorant indicators are given in Supporting Information, Table S1.

**Preparation of Formulations.** The sol–gel-colorant solutions were prepared by acid catalyzed hydrolysis of solutions containing

- (5) Meier, D. C.; Evju, J. K.; Boger, Z.; Raman, B.; Benkstein, K. D.; Martinez, C. J.; Montgomery, C. B.; Semancik, S. *Sens. Actuators, B* **2007**, *121*, 282–294.
- (6) (a) Rakow, N. A.; Suslick, K. S. *Nature* **2000**, *406*, 710–713. (b) Rakow, N. A.; Sen, A.; Janzen, M. C.; Ponder, J. B.; Suslick, K. S. *Angew. Chem., Int. Ed.* **2005**, *44*, 4528–4532. (c) Janzen, M. C.; Ponder, J. B.; Bailey, D. P.; Ingison, C. K.; Suslick, K. S. *Anal. Chem.* **2006**, *78*, 3591–3600. (d) Zhang, C.; Suslick, K. S. *J. Am. Chem. Soc.* **2005**, *127*, 11548–11549. (e) Zhang, C.; Bailey, D. P.; Suslick, K. S. *J. Agric. Food Chem.* **2006**, *54*, 4925–4931. (f) Zhang, C.; Suslick, K. S. *J. Agric. Food Chem.* **2007**, *55*, 237–242. (g) Feng, L.; Musto, C. J.; Suslick, K. S. *J. Am. Chem. Soc.* **2010**, *132*, 4046–4047.

- (7) (a) Lim, S. H.; Musto, C. J.; Park, E.; Zhong, W.; Suslick, K. S. *Org. Lett.* **2008**, *10*, 4405–4408. (b) Musto, C. J.; Lim, S. H.; Suslick, K. S. *Anal. Chem.* **2009**, *81*, 6526–6533. (c) Lim, S. H.; Kemling, J. W.; Feng, L.; Suslick, K. S. *Analyst* **2009**, *134*, 2453–2457.
- (8) (a) Lim, S. H.; Feng, L.; Kemling, J. W.; Musto, C. J.; Suslick, K. S. *Nat. Chem.* **2009**, *1*, 562–567. (b) Feng, L.; Musto, C. J.; Kemling, J. W.; Lim, S. H.; Suslick, K. S. *Chem. Commun.* **2010**, *46*, 2037–2039.
- (9) Suslick, B. A.; Feng, L.; Suslick, K. S. *Anal. Chem.* **2010**, *82*, 2067–2073.
- (10) (a) Podbielski, H.; Ulatowska-Jarza, A.; Muller, G.; Eichler, H. J. *Optical Chemical Sensors*; Springer: Erice, Italy, 2006. (b) Dunbar, R. A.; Jordan, J. D.; Bright, F. V. *Anal. Chem.* **1996**, *68*, 604–610. (c) Jeronimo, P. C. A.; Araujo, A. N.; Montenegro, M. *Talanta* **2007**, *72*, 13–27. (d) Rottman, C.; Grader, G.; De Hazan, Y.; Melchior, S.; Avnir, D. *J. Am. Chem. Soc.* **1999**, *121*, 8533–8543.
- (11) (a) Steumpfle, A. K.; Howells, D. J.; Armour, S. J.; Boulet, C. A. *Final Report of International Task Force-25: Hazard From Toxic Industrial Chemicals*; US GPO: Washington, DC, 1996. (b) Armour, S. J. *International Task Force 40: Toxic Industrial Chemicals (TICs)-Operational and Medical Concerns*; US GPO: Washington, DC, 2001.

**Table 1. List of Toxic Industrial Chemicals at Their IDLH (Immediately Dangerous to Life or Health) and PEL (Permissible Exposure Limit) Concentrations**

TIC	IDLH (ppm)	PEL (ppm)
ammonia	300	50
arsine	3	0.05
chlorine	10	1
diborane	15	0.1
dimethylamine	500	10
fluorine	25	0.1
formaldehyde	20	0.75
hydrogen chloride	50	5
hydrogen cyanide	50	10
hydrogen fluoride	30	3
hydrogen sulfide	100	20
hydrazine	50	1
methylamine	100	10
methyl hydrazine	20	0.2
nitric acid	25	2
nitrogen dioxide	20	5
phosgene	2	0.1
phosphine	50	0.3
sulfur dioxide	100	5
trimethylamine	200	10

commercially available silane precursors (e.g., tetraethoxysilane (TEOS), methyltriethoxysilane (MTEOS), phenethyltrimethoxysilane, and octyltriethoxysilane (octyl-TEOS)). After hydrolysis, the resulting solutions were added to the selected chemically responsive indicators. In order to design immobilization matrixes based on ormosils, combinations of TEOS with trialkoxysilanes were tested. Phenethyltrimethoxysilane was used with TEOS to immobilize all of the porphyrins and metalloporphyrins used in the array, while TEOS mixed with MTEOS and octyl-TEOS were used in the cases of acid and base treated indicators, respectively.

**Array Printing.** Final ormosil formulations with the colorants were loaded into a 36-hole Teflon ink well. Sensor arrays were printed using an array of 36 floating slotted pins (which delivered approximately 130 nL each; V&P Scientific, San Diego) by dipping into the ink well and transferring to the polyethylene terephthalate (PET) film. Robotic printing used an ArrayIt NanoPrint LM60 Microarray Printer. Once printed, the sol-gel was allowed to set under a slow stream of nitrogen for at least 3 days before any sensing experiments were performed.

**Experimental Procedures. Safety.** All gas streams containing toxic industrial chemicals (TICs) are, by definition, toxic. All handling of such gases must be done in a well ventilated fume hood; all exit flows of such gases should be passed through a treatment bubbler (e.g., base, acid, or bleach) as appropriate. Risk can be minimized by the purchase of premixed gases containing only concentrations of TICs a few times the IDLH (immediately dangerous to life or health).

**Gas Dilution.** Gas streams containing the TICs at their IDLH, PEL (permissible exposure limit), or lower concentrations were prepared by mixing the analyte stream with dry and wet nitrogen gas. MKS digital mass flow controllers (MFCs) were used to achieve the desired concentrations and relative humidity (RH), as shown in Supporting Information, Figure S1. The serial dilution apparatus could produce precise analyte concentrations down to ~0.01% of the initial gas tank concentration. Importantly, gas stream concentrations and relative humidity were confirmed by in-line analysis using Fourier transform infrared spectroscopy (FT-

IR) in real time using a MKS multigas analyzer (model 2030). The independent in-line analysis of tank gases was found to be essential because premixed tanks of these reactive gases at the low concentrations used here (typically four times the IDLH) did not generally retain their original certified concentrations. Fluorine, chlorine, hydrazine, nitric acid, and HF at their IDLH concentrations were confirmed using Dräger detector tubes (Dräger Safety, Inc.).

**Digital Imaging and Data Analysis.** For all sensing experiments, imaging of the arrays was performed using a flatbed scanner (Epson Perfection V200). The before-exposure image was acquired after 2 min of exposure to 50% relative humidity N<sub>2</sub> flow at 500 sccm. It should be noted that compressed air and air containing nominal concentrations of carbon dioxide (350–400 ppm) were also evaluated and showed identical results. After-images were acquired after every minute of exposure to the analyte with the same gas flow rates. Difference maps were obtained by taking the difference of the red, green, and blue (RGB) values from the center of every indicator spot (~300 pixels) from the “before” and “after” images; all difference maps shown in figures are averages of multiple (typically seven) trials, but the statistical analyses always use all individual trials. Digitization of the color differences were performed using Adobe Photoshop or a customized software package, ChemEye. To eliminate the possibility of subtraction artifacts caused by acquisitions near the spot edge, only the spot center (typically 50% of the total spot size) was included in the calculation. Chemometric analyses were carried out on the color difference vectors using the Multi-Variate Statistical Package (MVSP v. 3.1, Kovach Computing); in all cases, minimum variance (Ward’s method) was used for hierarchical cluster analysis (HCA).

**Temperature Experiments.** To achieve temperature control of the array cartridge and incoming gas stream, a one liter glass beaker was placed on top of the array containing heated or cooled liquid; a mixture of dry ice and 2-propanol was used for cooling, and hot tap water was used for heating. The temperature of the gas inside the cartridge was monitored by the outgoing gas stream using an Omega HH11 thermocouple and was held at the desired temperature with a variance no greater than  $\pm 0.5$  °C throughout the experiment. All temperature experiments were performed at 50% relative humidity (which was calibrated according to standard temperature–humidity curves vs temperature).

**Humidity Experiments.** Relative humidity was controlled by mixing dry nitrogen with humidity-saturated nitrogen (100% relative humidity, generated by bubbling nitrogen through water). A reference image was collected after equilibration with 50% relative humidity; arrays were then exposed to various humidity concentrations with 500 sccm gas flow for 10 min with data acquisition every minute.

**Cycling Experiments.** The colorimetric sensor arrays were exposed to nitrogen (50% relative humidity) for 5 min, and then, the gas stream switched from IDLH to PEL and back every 10 min with data acquisition every minute.

## RESULTS AND DISCUSSION

In any optical sensing platform, the matrix of the sensor may have several desirable or necessary features: (1) the responsive colorant and all additives need to remain fully dispersed or dissolved in the matrix so that the analyte can gain access to the



colorant, (2) the analyte should be able to diffuse through the matrix to the indicator in a reasonably rapid time frame (e.g., seconds), (3) the matrix material should be chemically and physically stable so that the array has good shelf life, and (4) the matrix should not have any significant color or luminescence in the region of the spectrum being studied.<sup>12</sup> On the basis of these requirements, sol-gel silica is an excellent matrix for a variety of organic and inorganic colorants because of its high surface area, good stability over a fairly wide range of pH (excluding alkaline), relative inertness in many environments, and transparency in the UV-visible spectrum. The versatility of the matrix is substantially enhanced by the use of organically modified siloxanes, as discussed earlier.<sup>10</sup> Importantly, we have developed ormosil formulations that permit printing on simple polymer surfaces, permitting easy packaging of the sensor array into a self-sealing cartridge with minimal dead space.<sup>8</sup>

**Array Design.** As discussed earlier, the required indicator classes for our colorimetric sensor array include metal ion containing dyes (e.g., metalloporphyrins), pH indicators, vapo-chromic/solvatochromic dyes, and redox sensitive metal salts. The specific colorants incorporated into the ormosil formulations are given in Supporting Information, Table S1.

Because of their open coordination sites for axial ligation, their large spectral shifts upon ligand binding, and their high extinction coefficients, metalloporphyrins are a natural choice for the detection of metal-ligating vapors (i.e., Lewis bases). The importance of including metal-containing sensors is further highlighted by recent indications that the mammalian olfactory receptors<sup>13</sup> are probably metalloproteins.<sup>14</sup> Traditional pH indicators are useful, of course, for Brønsted acidic and basic analytes, and in addition, they can be responsive to Lewis (i.e., electron pair donor/acceptor) interactions as well; it has long been known, for example, that pH indicators in water are susceptible to “interference” from dissolved organics.<sup>15</sup> Vapochromic indicators are more general purpose and can provide for subtle discrimination among similar analytes of the same chemical class. Finally, we have added various metal salts to our array for the specific detection of some analytes, such as arsine and phosphine, which react forming metal nanoparticles and acidic byproducts that are detected by incorporated pH indicators.

**Data Analysis.** Color difference maps for the arrays were generated by subtraction of the digital image of the array before exposure from the image after exposure. Every spot in the array is uniquely described by its RGB color values; for an eight-bit color scanner, these values range from 0 to 255. Thus, every analyte response is represented digitally by a 108-dimensional vector (i.e., the changes in the red, green, and blue values of each of the 36 spots:  $\Delta R$ ,  $\Delta G$ ,  $\Delta B$ ). In principal, the range of these color changes can range from  $-255$  to  $+255$  for eight-bit color. A color difference map is useful for visualization of these data and is easily generated by taking the absolute value of the  $\Delta R$ ,  $\Delta G$ ,

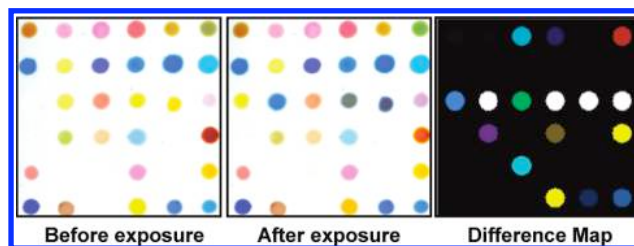


**Figure 2.** Images of the 36-dye colorimetric sensor array before exposure, after 2 min of exposure to ammonia at its IDLH concentration at 298 K and 50% relative humidity and the generated color difference map.

and  $\Delta B$  (Figure 2). The difference maps are usually not displayed over the full 0–255 range as changes in RGB values rarely span the entire 256 range; rather, for improved visualization, the color palette of the difference maps are expanded, for example, from 4 to 8 bits per color (i.e., the RGB range of 4–19 is expanded to 0–255, as in Figure 2). For all quantitative and statistical comparisons, of course, we work directly from the original digital data (which has been provided in the Supporting Information).

#### Discrimination of Toxic Industrial Chemicals at IDLH Concentrations.

We have extensively tested our colorimetric sensor arrays against 20 TICs at their IDLH concentrations at 50% relative humidity. Most of the TICs can be identified at their IDLH concentrations from the array color change in a matter of seconds, and >90% of total response is observed in less than 2 min, as shown in the Supporting Information, Figure S2. For some pigments, the response time can be slightly longer, but even in these cases, the color-change pattern is distinctive and easily recognized at 2 min. The arrays were exposed to a gas mixture produced from either premixed, certified gas cylinders or saturated vapor, using digital mass flow controllers. The gas compositions were assayed by inline analysis in real time using an FT-IR multigas analyzer for most analytes or by Dräger detector tubes in the few cases where FT-IR could not be used (e.g., homonuclear diatomics such as chlorine and fluorine).

The colorimetric sensing arrays were fully successful at detecting and identifying TICs at their IDLH concentrations as demonstrated by the difference maps of the TICs shown in Figure 3. Even by eye, without statistical analysis, the array response to each TIC is represented by a unique pattern. Excellent discrimination among a very wide range of analytes was observed. Furthermore, different chemical classes were easily differentiated: the color patterns of compounds (e.g., amines vs acids vs fluorine/chlorine vs arsine/phosphine, etc.) were very different from one another and were easily distinguishable.

Septuplicate data were acquired to probe the reproducibility of the array response to each analyte. The high dispersion of the colorimetric sensor array data requires a classification algorithm that uses the full dimensionality of the data. Hierarchical cluster analysis (HCA) provides the simplest approach that assumes no statistical model (as opposed to linear discriminant analysis (LDA), for example). HCA is based on the grouping of the analyte vectors according to their spatial distances in their full vector space.<sup>16</sup> The main purpose of HCA is to divide the analytes into discrete groups based on the characteristics of their respective responses. HCA forms dendrograms based on the clustering of our array response data in the 108 dimensional  $\Delta RGB$  color space, as shown

(12) Mohr, G. J. In *Optical Chemical Sensors*; Baldini, F., Ed.; Springer: Erice, Italy, 2006; pp 297–321.

(13) Hawkes, C. H.; Doty, R. L. *The Neurology of Olfaction*; Cambridge University Press: Cambridge, U.K., 2009.

(14) (a) Wang, J.; Luthe-Schulten, Z. A.; Suslick, K. S. *Proc. Natl. Acad. Sci. U.S.A.* **2003**, *100*, 3035–3039. (b) Zarzo, M. *Rev. Environ. Sci. Biotechnol.* **2007**, *82*, 455–479.

(15) Kolthoff, I. M. *Acid-Base Indicators*; MacMillan Co: New York, 1937; pp 197–215; translated by Rosenblum, C.

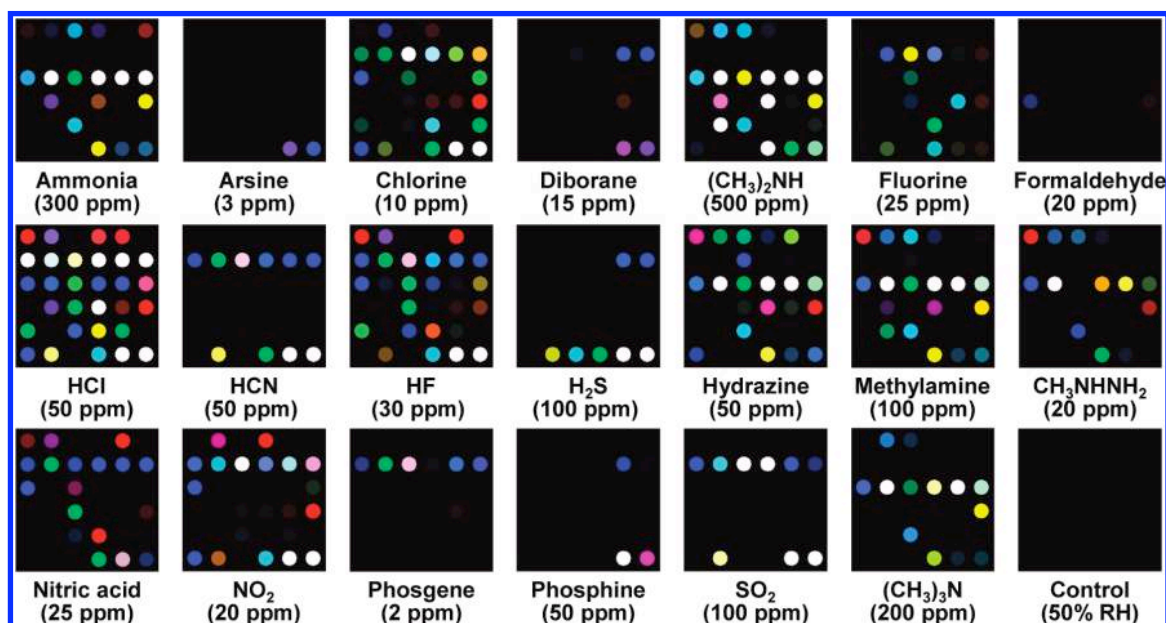


**Figure 3.** Color change profiles of representative toxic industrial chemicals at their IDLH concentration after 2 min of exposure. For purposes of visualization, the color range of these difference maps is expanded from 4 to 8 bits per color (RGB range of 4–19 expanded to 0–255).

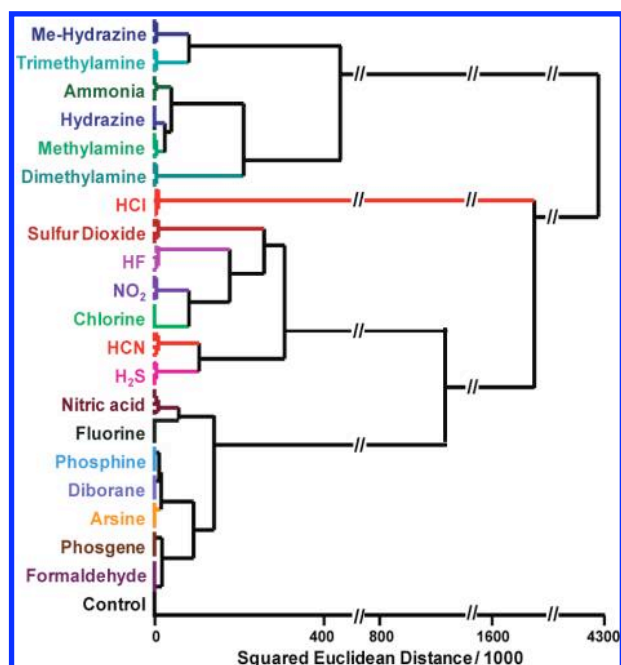


**Figure 4.** Hierarchical cluster analysis for 20 TICs at IDLH concentrations and a control. All experiments were performed in septuplicate, and the HCA analysis uses all 147 individual trials; no confusions or errors in clustering were observed in 147 trials, as shown.

in Figure 4. Remarkably, in septuplicate trials, all 20 TICs and a control were accurately identified against one another with no error or misclassifications out of 147 cases.

While the color differences of the array generate 108-dimensional vectors (for a  $6 \times 6$  array), we know that these are not fully independent dimensions. In order to probe the effective

dimensionality of our data, we first employed principal component analysis (PCA)<sup>16</sup> to evaluate the variance in the array response among the range of analytes. The eigenvector of each principal component is defined by a linear combination of the response vectors (i.e., the 108-dimensional difference vector) so as to maximize the amount of variance in as few dimensions as possible. PCA is a model-free (i.e., “unsupervised”) statistical model that is widely used to reduce the dimensionality of data sets that consist of a large number of interrelated measurements. Generally, PCA for most prior electronic nose technologies is dominated by only two or at most three independent dimensions; in fact, there is usually a single dominant dimension which accounts for >90% of the total discrimination and which roughly corresponds to sensor hydrophobicity (i.e., the dominant factor in adsorption on metal oxide surfaces or sorption into polymer films). The colorimetric sensor array, in contrast, is not limited to weak, nonselective interactions but rather employs a variety of stronger intermolecular interactions between the nanoporous pigments and the analytes. The colorimetric sensor array, therefore, is able to explore a much larger volume of “chemical-properties space” probed by our choice of chemoresponsive nanoporous pigments. As shown in Supporting Information Figure S3A, based on 147 trials at IDLH concentration, the PCA of our colorimetric sensor array required 11 dimensions for 90% of the discriminatory power and 17 dimensions for 95%. By probing a much wider range of chemical interactions, we have dramatically increased the dispersion of our sensor array. It is this increased dimensionality that permits us to discriminate among very closely related analytes.

To further evaluate the ability of the colorimetric sensor array to discriminate among different TICs, we also performed a linear discriminant analysis (LDA) of the 147 trials. LDA is a supervised linear classifier statistical model and one of the prevailing methods for classification analysis of high dimensionality data sets.<sup>16</sup> Given the 108 measurements for each analyte, the total variation of the measurements can be decomposed into two parts: the between-group variation and the within-group variation. LDA finds linear

(16) (a) Hasswell, S. *Practical Guide to Chemometrics*; Dekker: New York, 1992. (b) Scott, S. M.; James, D.; Ali, Z. *Microchim. Acta* **2007**, *156*, 183–207. (c) Johnson, R. A.; Wichern, D. W. *Applied Multivariate Statistical Analysis*, 6th ed.; Prentice Hall: Upper Saddle River, NJ, 2007. (d) Hair, J. F.; Black, B.; Babin, B.; Anderson, R. E.; Tatham, R. L. *Multivariate Data Analysis*, 6th ed.; Prentice Hall: Upper Saddle River, NJ, 2005.

combinations of the measurements (“directions”) that maximize the between-group variation relative to the within-group variation. More specifically, LDA finds low dimensional projections of the original data that can best separate the analytes into their known classes. When the classification error rates for LDA as a function of increasing numbers of principal directions (using a “leave-one-out” cross-validation) was examined, the error rate becomes zero (with  $n = 147$ ) at ten directions (Supporting Information Figure S3B). Thus, LDA gave excellent general agreement with the PCA with respect to the overall dimensionality of the sensor array data. As with HCA, the LDA classification is exceptionally accurate: using a leave-one-out cross-validation, the misclassification rate is  $<0.7\%$  (i.e., no errors among 147 trials) with 10 LDA directions.

**Discrimination of Toxic Industrial Chemicals at PEL Concentrations.** At a sufficiently low dose and short exposure, acute toxicity will diminish nearly completely (as Paracelsus observed 500 years ago, the dose makes the poison.). Even at their permissible exposure limits (PEL), however, TICs may still cause serious health effects after multiple low-level exposures. Thus, the ability to monitor low concentrations of these analytes is an important goal.

Chemists have no equivalent of the physicists’ radiation badge: there is no readily available general purpose method to easily measure the low levels of personal exposure that workers may receive to the diverse range of volatile TICs used in laboratories, manufacturing facilities, or general storage areas.<sup>17,18</sup> There are, of course, numerous conventional methods<sup>18</sup> for the detection of gas phase hazardous chemicals, including GC/MS,<sup>19</sup> ion mobility spectrometry (IMS),<sup>20</sup> electronic nose technologies,<sup>1</sup> and colorimetric detectors tailored to specific single analytes.<sup>18</sup> Most such detection technologies, however, suffer from severe limitations: GC/MS is expensive and nonportable; IMS has limited chemical specificity; electronic nose technologies have restricted selectivity, sensitivity, and resistance to environmental interference (e.g., humidity); and single analyte detectors are too specific for multiple possible exposures.

As an approach to monitoring low levels of exposures to multiple possible toxicants, we tested our colorimetric sensor array against 20 TICs at their PEL concentrations. Although 2 min of exposure is sufficient to obtain a reliable response from most of the TICs at their PEL concentrations, the arrays were exposed to a diluted gas mixture for 5 min in order to more fully equilibrate the array response (Supporting Information, Figure S2). As shown in Figure 5, the HCA indicates that all 20 TICs and a control were accurately identified against one another with no errors or misclassifications out of 147 cases. Even weakly responding gases

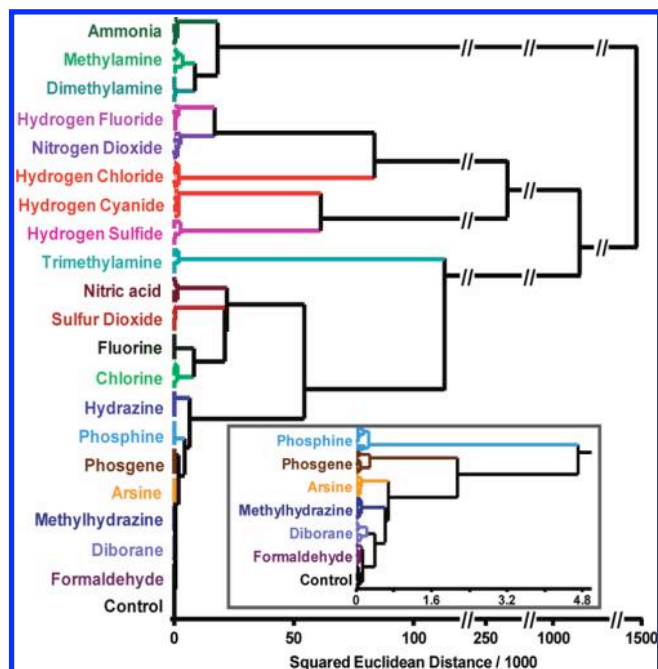


**Figure 5.** Hierarchical cluster analysis for 20 TICs at PEL concentrations and a control; RH = 50%. All experiments were performed in septuplicate; no confusions or errors in classification were observed in 147 trials, as shown.

gave discrete clusters without error (see inset of Figure 5). We again used PCA to gain a measure of the dimensionality of the data set collected at PEL for these 20 TICs. On the basis of the 147 trials of 20 TICs and a control, PCA of our colorimetric sensor array requires 17 dimensions for 90% of total variance and 26 dimensions for 95% (Supporting Information, Figure S3); using a leave-one-out cross-validation, LDA gave a minimum misclassification rate of  $<1\%$  (i.e., one error in 147 leave-one-out trials) with 11 LDA directions (Supporting Information, Figure S3). This extremely high dispersion is consistent with the similar results discussed above for the array response at IDLH and reflects the wide range of chemical-property space being probed by our choice of chemically responsive pigments, even at very low concentrations.

**Discrimination of Toxic Industrial Chemicals as a Function of Concentration.** For most analytes, the response of these colorimetric sensor arrays is based primarily on equilibrium interactions between the array pigments and the analytes. As a result, different concentrations of the same analyte give different array responses. By combining the data sets at IDLH and at PEL, we can clearly differentiate the array responses to the same analytes at different concentrations. Clustering analysis for the full set of IDLH and PEL databases can be seen in the Supporting Information, Figure S4.

More generally, each concentration of a TIC has a separate unique pattern. As examples, color change profiles for three different analytes,  $\text{Cl}_2$ ,  $\text{NH}_3$ , and  $\text{SO}_2$ , as a function of concentration are illustrated in Figure 6. Even at only 20% of their PELs, there is no confusion among the analytes at different concentrations, as can be seen with simple visual comparison.

**Limits of Detection and Limits of Recognition.** For the colorimetric sensor array, the limit of detection (LOD) is analyte dependent and reflects the inherent chemical reactivity of each analyte with the various colorants in the array. We can estimate

- (17) (a) Byrnes, M. E.; King, D. A.; Tierno, P. M., Jr. *Nuclear, Chemical, and Biological Terrorism-Emergency Response and Public Protection*; CRC Press: Boca Raton, FL, 2003. (b) Lauwerys, R. R.; Hoet, P. *Industrial Chemical Exposure: Guidelines for Biological Monitoring*, 3rd ed.; CRC Press: Boca Raton, FL, 2001. (c) Janata, J. *Annu. Rev. Anal. Chem.* **2009**, *2*, 321–331.
- (18) (a) Chou, J. *Hazardous Gas Monitors: A Practical Guide to Selection, Operation and Applications*; McGraw-Hill: New York, 2000; (b) McDermott, H. J. *Air Monitoring for Toxic Exposure*; John Wiley & Sons: Hoboken, NJ, 2004. (c) Janata, J. *Principles of Chemical Sensors*, 2nd Ed. Springer: New York, 2009.
- (19) Hübschmann, H.-J. *Handbook of GC/MS: Fundamentals and Applications*; Wiley-VCH: Weinheim, 2009.
- (20) Eiceman, G. A.; Karpas, Z. *Ion Mobility Spectrometry*; CRC Press: Boca Raton, FL, 2005.



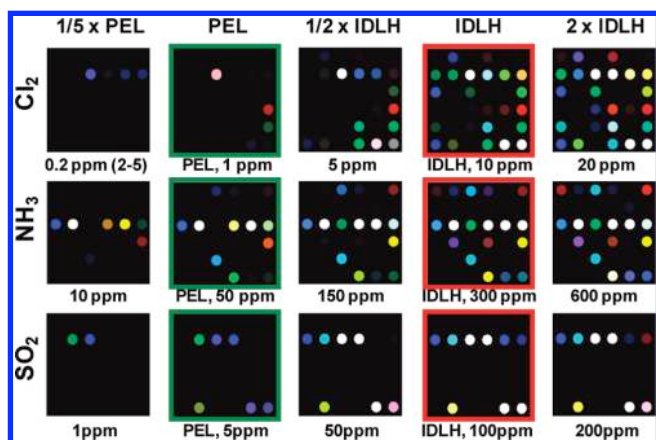


**Figure 6.** Effect of concentration on array response to  $\text{NH}_3$ ,  $\text{SO}_2$ , and  $\text{Cl}_2$  after 2 min exposure. For purposes of visualization, the color range of these difference maps is expanded from 4 to 8 bits per color (RGB range of 4–19 expanded to 0–255), except for weaker responding TICs ( $\text{Cl}_2$  at 0.2 ppm; RGB range of 2–5 expanded to 0–255).

the LOD for each TIC by extrapolating from the observed array response at their respective PELs. We have defined a conservative LOD for our array response as the TIC concentration needed to give three times the S/N vs background for the sum of the three largest responses among the 108 array color changes. Supporting Information Table S2 lists our estimated limit of detection for each analyte extrapolated from their 5 min PEL response; remarkably, the LODs of the 20 TICs are in the low ppb regime and, on average, only 4.1% of the TICs' respective PELs.

A limit of detection only indicates the concentration at which the sensor first responds to an analyte (at three times the background S/N) but does not necessarily indicate the capability to discriminate among analytes. The limit of recognition (LOR) is a less well-defined parameter that depends upon the group of analytes among which one wishes to differentiate. In order to generate a rough estimate of LOR of our array, we examined a subset of five TICs at concentrations far below their PELs. As shown in Figure 7, HCA of these five TICs at 5% of the PEL was without misclassification in 30 quintuplicate trials.

**Reversibility and Cycling Experiments.** The colorimetric sensor arrays are meant to be disposable but not necessarily single use, in analogy to an electrical fuse. As a “chemical fuse”, an array may be used to continuously monitor analyte concentrations, and as long as those concentrations fluctuate within some range, the array continues to function. After exposure to very high concentrations or to very aggressive analytes, the array is “blown” and must be replaced. As illustrated in Figure 8 for  $\text{SO}_2$ , the colorimetric sensor array cycled reproducibly between the IDLH and PEL concentrations for many analytes. Equilibrium response is achieved within 2 min of switching between concentrations. The reversibility of the array depends on the type of chemical reaction between the indicators and analytes. For highly aggressive analytes (e.g., chlorine, which bleaches the array's colorants irreversibly), the array cannot be recycled, as demonstrated in Figure 7B.

**Humidity, Temperature, and Interferences.** The interference of atmospheric humidity on sensor performance is a serious problem with most array-based gas sensing technologies. The high concentration of water vapor in the environment and (even more

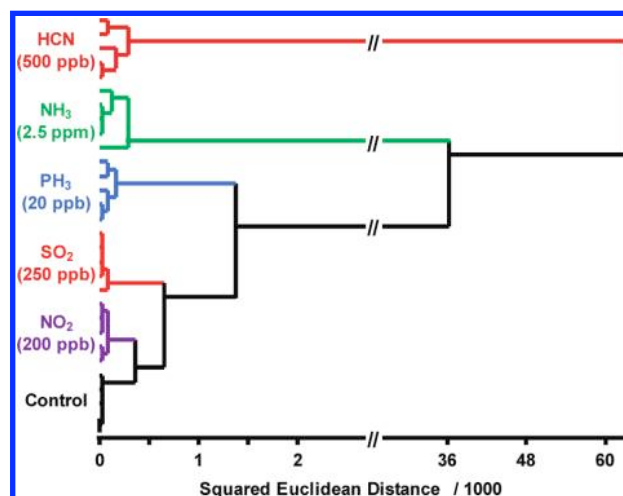


**Figure 7.** Low concentration tests of five TICs at ~5% of their PELs after 10 min exposure. All experiments were performed in quintuplicate; no confusions or errors in classification were observed in 30 trials, as shown.

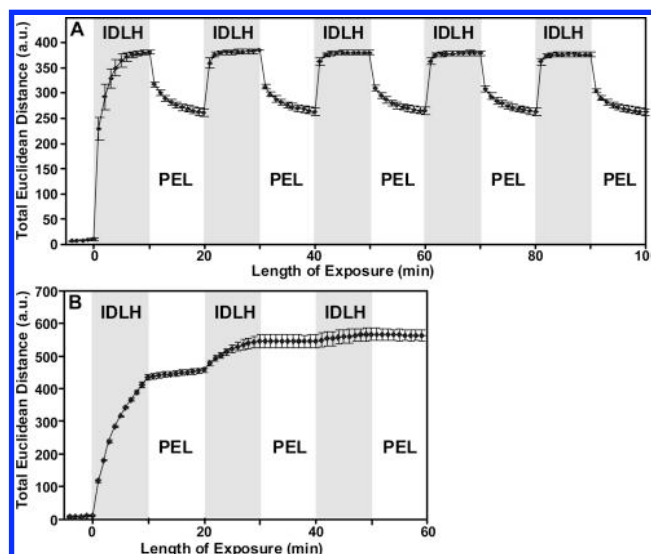


**Figure 8.** Reversibility of colorimetric sensor array response. (A)  $\text{SO}_2$  exposure of the array from  $\text{N}_2$  to the IDLH (100 ppm) level and then cycled between IDLH and PEL (5 ppm), showing excellent reproducibility. (B)  $\text{Cl}_2$  exposure of the array from  $\text{N}_2$  to IDLH (10 ppm) and then cycled between IDLH and PEL (1 ppm). Data acquired every 1 min; average of three trials is shown with standard deviations. The total Euclidean distance is simply the total length of the 108-dimensional color difference vector, i.e., the total array response.

importantly) its large range on a daily basis make the accurate detection of analytes at low concentrations exceptionally challenging. Typical water vapor concentrations in the environment range from <300 to >73 000 ppm (i.e., 10% RH at  $-10^\circ\text{C}$  to 90% RH at  $40^\circ\text{C}$ ); even a very low level of interference from water vapor is intolerable if one wishes to detect sub-ppm concentrations of other analytes. It should be no surprise that sensitivity to changes in humidity has been a very serious weakness in prior electronic nose technologies.

We have incorporated hydrophobic dyes in hydrophobic matrixes into our colorimetric sensor array, thus rendering the sensor array much less sensitive to changes in humidity. Our nanoporous pigment sensing arrays were essentially unresponsive

to changes in relative humidity, as seen in Supporting Information, Figure S5. The arrays were equilibrated at 50% RH for 2 min and, then, exposed to water vapor from 10% to 90% RH for 5 or 10 min. No detectable response to variations in humidity was observed. The effect of humidity on the array response to TICs was also evaluated. Two examples are shown in Supporting Information Figure S6A, where  $\text{NH}_3$  and  $\text{SO}_2$  show virtually the same color change pattern under four different relative humidity concentrations. HCA shows clear discrimination between  $\text{SO}_2$  and  $\text{NH}_3$  independent of relative humidity (Supporting Information, Figure S7A).

Sensor arrays that are mobile and employed "in the field" will encounter not only a large range of relative humidity but also wide temperature ranges. It should be noted that in realistic sampling conditions (10–40 °C) very little change in the difference maps is observed among the analytes tested (Supporting Information, Figure S6B). HCA of the temperature data shows tight clustering for each analyte over the temperature range, with large separation between the two analyte clusters (Supporting Information, Figure S7B).

In real world use, one must also be concerned about interference, in terms of both false positives from a harmless vapor and false negatives from masking of a TIC by some harmless vapor. The distinctive property of nearly all TICs is their high chemical reactivity: a harmless vapor, essentially by definition, does not have high chemical reactivity. Because the response of the colorimetric sensor array is based on chemical reactivity, potential interfering agents are generally not problematic. The colorimetric sensor array has been tested extensively against nine common potential interfering agents: second hand smoke, diesel fuel exhaust, gasoline exhaust, toluene, WD-40, Klean-Strip stripper, Windex, Fantastik, and Clorox Bleach, each at concentrations of 1% and 2% of their saturated vapor at room temperature and 50% RH. As shown in Supporting Information Figure S8, after 5 min of exposure, the sensor array gave no response to all interfering agents except for Windex, which contains ammonia well above its IDLH and is, therefore, truly a TIC and not an interfering agent.

**Shelf Life and Reproducibility.** To evaluate the shelf life of our colorimetric sensor array, four representative TICs ( $\text{NH}_3$ ,  $\text{SO}_2$ ,  $\text{Cl}_2$ , and  $\text{H}_2\text{S}$ ) were tested as a function of aging of the printed arrays. Arrays were stored in polyethylene bags under  $\text{N}_2$  for 1, 2, 4, 6, and 12 weeks. As shown in Supporting Information Figures S9 and S10, storage time has essentially no effect on the array response: no confusions or errors in classification were observed among these 60 trials (triplicate trials of four TICs over five time periods). The difference maps are shown in the Supporting Information, Figure S12.

As shown earlier, septuplicate trials of our colorimetric sensor arrays against the 20 TICs at both IDLH and PEL concentrations, excellent reproducibility of array response is observed within each batch of printings. Just as important, however, is the reproducibility of the array from printing batch to batch. We conducted a series of experiments to specifically test the array response from two different batches printed on different days. Eight TICs ( $\text{NH}_3$ ,  $\text{SO}_2$ ,  $\text{Cl}_2$ ,  $\text{H}_2\text{CO}$ ,  $\text{Cl}_2\text{CO}$ ,  $\text{B}_2\text{H}_6$ ,  $\text{PH}_3$ , and  $\text{H}_2\text{S}$ ) were selected as an example of each class of analyte. As seen in Supporting Information Figure S12B, excellent batch-to-batch reproducibility is also observed: the HCA of septuplicate trials of each batch for each analyte yields no misclassifications or confusions among the eight analytes and a control.

## CONCLUSIONS

We have designed a simple, disposable colorimetric sensor array of nanoporous pigments that is capable of fast, sensitive detection of a wide range of toxic gases. By immobilizing chemically responsive indicators within nanoporous sol-gel matrixes, we have tested a colorimetric sensor array for the detection of 20 toxic industrial chemicals. The sensor array is able to discriminate without error among these 20 TICs at their permissible exposure limit (PEL) concentrations, with estimated limits of detection in the few ppb range (i.e., well below the PEL). Classification analysis reveals that the colorimetric sensor array has an extremely high dimensionality and, consequently, the ability to discriminate among large numbers of TICs over a wide range of concentrations. The array performs well in the presence of various common potential interfering agents and has shown excellent stability and reproducibility. Although we are not yet at the point of a truly wearable personal monitor for multiple toxic gases, we do have a hand-held array reader at the prototype stage of development,<sup>5</sup> and further miniaturization is under development.

## ACKNOWLEDGMENT

This work was supported through the NIH Genes, Environment, and Health Initiative through Award U01ES016011.

## SUPPORTING INFORMATION AVAILABLE

Tables of indicators and analytes, additional figures, and array response database (Supporting Information Tables S3 and S4). This material is available free of charge via the Internet at <http://pubs.acs.org>.

Received for review August 10, 2010. Accepted September 30, 2010.

AC1020886